Acta Crystallographica Section A
Foundations of Crystallography
ISSN 0108-7673

Received 22 July 2010
Accepted 7 September 2010

Double-slit dynamical diffraction of X-rays in ideal crystals (Laue case)

Minas K. Balyan

Yerevan State University, Faculty of Physics, Department of Solid State Physics, Solid State Physics Research Laboratory, Armenia, and Yerevan State University, 'Centre for the Advancement of Natural Discoveries Using Light Emission (Candle)', Research Institute at YSU, Armenia.
Correspondence e-mail: mbalyan@ysu.am

The theoretical investigation of double-slit dynamical X-ray diffraction in ideal crystals shows that, on the exit surface of crystals, interference fringes similar to Young's fringes are formed. An expression for the period of the fringes was obtained. The visibility of the fringes depending on temporal and spatial coherent properties of the incident beam is studied. The polarization state of the incident beam also affects the visibility of the fringes, which in turn depends on the size of the slits. The deviation from Bragg's exact angle causes a shift of the fringes and can also affect the amplitude of the intensity. One of the parameters on which the visibility of the fringes depends is the source–crystal distance. The proposed scheme can be used as a Rayleigh X-ray interferometer. Use of the scheme as a Michelson X-ray stellar interferometer is also possible.

1. Introduction

The dynamical diffraction of X-rays in crystals essentially depends on the degree of perfection of the crystals and on the parameters of the incident beam. The diffraction of monochromatic spatially inhomogeneous beams is described by Takagi's equations (Takagi, 1969). The general method for solving these equations was given by Slobodetskii *et al.* (1968), Authier & Simon (1968) and Uragami (1969). The equations of dynamical diffraction are applicable in cases where the wavelength is much smaller than the characteristic size of the inhomogeneity. The diffraction of an X-ray beam restricted by a receiving slit has been studied theoretically and experimentally (Kato & Lang, 1959; Homna *et al.*, 1966; Kato, 1961*a*,*b*, 1968*a*,*b*; Authier *et al.*, 1968; Hart & Milne, 1968; Kohra & Kikuta, 1968; Slobodetskii & Chukhovskii, 1970).

It is interesting to investigate the dynamical diffraction of an incident wave which is restricted by two slits. The interference fringes which are observed when the sizes of the slits are small compared with the distance between their centres and when the distance between the centres is small compared with the distance from the plane of the slits to the observation point are called Young's fringes. This is well known in optics (Born & Wolf, 2002). The corresponding experiment is called Young's double-slit experiment. Investigations in the X-ray region of the classic and virtual Young's experiment are presented by Leitenberger *et al.* (2001, 2004), Yamazaki & Ishikawa (2003), Leitenberger & Pietsch (2007), Tsuji *et al.* (2009) and Isakovic *et al.* (2010).

In this paper the theoretical investigation of X-ray double-slit Laue symmetric diffraction in ideal crystals using Green's function formalism is presented (Fig. 1). Based on the obtained equations it is shown that, on the exit surface of the crystal, fringes similar to Young's fringes in optics are formed. For the intensity distribution an analytical approximation is given. The results of this approximation are compared with the solution of numerical calculations. A formula for the period of the interference fringes is obtained. The visibility of the interference pattern is theoretically studied depending on the monochromatization degree of the incident beam and on the size of the source [the temporal coherence and spatial coherence, respectively, which are usually related to the longitudinal and transverse coherence lengths (Als-Nielsen & McMorrow, 2001)], the sizes of the slits, the deviation from Bragg's exact angle, the source–crystal distance and the state of polarization. For the scheme shown in Fig. 1, owing to the formation of the Borrmann triangle, the region of interference is larger than that for the classic X-ray double-slit experiment.

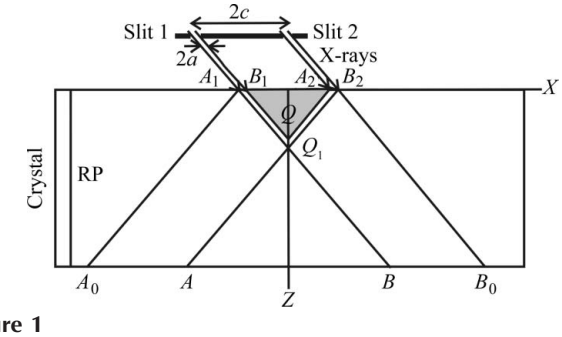

Figure 1
Scheme of double-slit dynamical diffraction of X-rays. 2*c*: distance between the centres of the slits; *OXZ*: the coordinate system. *O* is situated in the middle of the two slits, the *OX* axis is antiparallel to the diffraction vector **h** and *OZ* is perpendicular to the entrance surface. RP: reflecting planes.

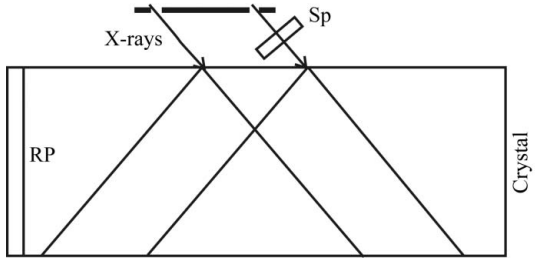

Figure 2
Scheme of the Rayleigh X-ray dynamical diffraction interferometer. Sp: specimen.

The scheme presented in Fig. 1 can be considered as an interferometer with division of the wavefront (Rayleigh interferometer). By placing a specimen in the way of one of the interfering beams and by measuring the shift of the interference fringes one can determine the refractive index of the specimen (Fig. 2). By using the scheme given in Fig. 1 the angular distance of two incoherent sources can be determined as in the case of the Michelson stellar interferometer in optics (Fig. 3).

2. Theory

The electric field of an arbitrary non-polarized incident wave can be described by the expression $\mathbf{E}^i(\omega, \mathbf{r})\exp(i\mathbf{Kr})$, where $\mathbf{E}^i$ is the slowly varying amplitude, ω is the frequency corresponding to wavelength λ, and $\mathbf{K}$ is the carrying wavevector of the incident beam. The direction of $\mathbf{K}$ is independent of wavelength and $\mathbf{K}^2 = (2\pi/\lambda)^2$. The glancing angle formed by $\mathbf{K}$ and the entrance surface of the crystal is $\pi/2 - \theta$, where θ is the angle between the wavevector $\mathbf{K}$ and the reflecting atomic planes (Fig. 1). A field of any frequency in the crystal is presented by the two-wave approximation as

$$\mathbf{E} = \mathbf{E}_0\exp(i\mathbf{K}_0\mathbf{r}) + \mathbf{E}_h\exp(i\mathbf{K}_h\mathbf{r}),$$

where $\mathbf{K}_0$ and $\mathbf{K}_h = \mathbf{K}_0 + \mathbf{h}$ are the wavevectors of the transmitted and diffracted fields, respectively, which for a certain wavelength satisfy Bragg's exact condition $\mathbf{K}_0^2 = \mathbf{K}_h^2 = k^2 = (2\pi/\lambda)^2$, $\mathbf{h}$ is the reciprocal-lattice vector satisfying the reflection condition $\mathbf{h} = -|\mathbf{h}|\mathbf{e}_x$, where $|\mathbf{h}| = 2k\sin\theta_0(\lambda)$, $k = 2\pi/\lambda$, $\theta_0(\lambda)$ is the Bragg exact angle for the wavelength λ, and $\mathbf{e}_x$ is the unit vector along the coordinate x. In the following, $\theta_0(\lambda) \rightarrow \theta_0$ (with the exception of §3.1.2). It should be noted that $|\mathbf{h}|$ is independent of the wavelength. $\mathbf{E}_0$ and $\mathbf{E}_h$ are the amplitudes of the electric fields of the transmitted and diffracted wave, respectively, for the same wavelength.

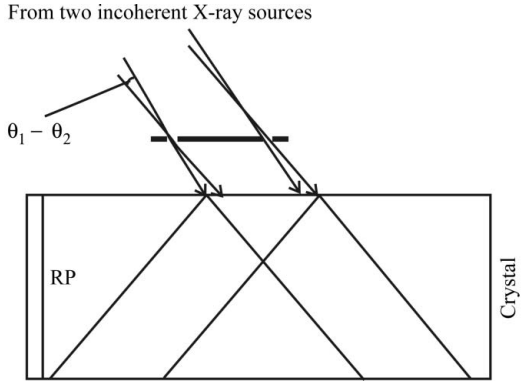

Figure 3
Scheme of the Michelson X-ray dynamical diffraction stellar interferometer.

The amplitudes satisfy Takagi's equations (Takagi, 1969) and continuity conditions on the entrance surface of the crystal ($z = 0$). For any state of the polarization it follows from the continuity condition on the entrance surface that $E^i(\omega, \mathbf{r})\exp(i\mathbf{Kr}) = E_0(\omega, \mathbf{r})\exp(i\mathbf{K}_0\mathbf{r})$ and, therefore, the amplitude E_0 on the entrance surface is

$$E_0 = E^i\exp(ik\cos\theta_0\Delta\theta x), \quad (1)$$

where $\Delta\theta = \theta - \theta_0$ is the deviation from the exact Bragg angle for given λ. The amplitude of the diffracted wave in the crystal in the symmetric Laue case can be presented by means of Green's function of dynamical diffraction as a convolution along the entrance surface of the crystal,

$$E_h = \int_{-\infty}^{+\infty} G(x - x', z)E^i(x')\exp(ik\cos\theta_0\Delta\theta x')\,\mathrm{d}x', \quad (2)$$

$$G(x, z) = ik\chi_h C J_0\left[\pi\cot\theta_0\left(z^2\tan^2\theta_0 - x^2\right)^{1/2}/\Lambda\right] \times \exp(ik\chi_0 z/2\cos\theta_0)H(z\tan\theta_0 - |x|)/4\sin\theta_0 \quad (3)$$

(Slobodetskii & Chukhovskii, 1970; Authier, 2001; Pinsker, 1982). Here χ_0, χ_h, $\chi_{\bar{h}}$ are the crystal dielectric susceptibility Fourier components corresponding to the zero and $\mathbf{h}$ reflections. Without loss of generality, for definiteness, it is assumed that $\chi_h = \chi_{\bar{h}}$, $\chi_{hr} = \chi_{\bar{h}r} < 0$, $\chi_{hi} = \chi_{\bar{h}i} > 0$, $\chi_{hi} \ll |\chi_{hr}|$, $\chi_{hi} \cong \chi_{0i} > 0$. $H(x)$ is the step function: $H(x) = 1$ if $x > 0$, $H(x) = 0$ if $x < 0$; J_0 is the zero-order Bessel function, $\Lambda = \lambda\cos\theta_0/C(\chi_h\chi_{\bar{h}})^{1/2}$ and C is the polarization factor: $C = 1$ for σ polarization and $C = \cos 2\theta_0$ for π polarization. The real part of Λ, *i.e.* $\Lambda_r = \mathrm{Re}\,\Lambda \simeq \lambda\cos\theta_0/C|\chi_{hr}|$ is the extinction length and $\Lambda_i = \mathrm{Im}\,\Lambda \simeq \Lambda_r\chi_{hi}/|\chi_{hr}|$ is concerned with absorption in the crystal. For the scheme given in Fig. 1,

$$E_h = \int_1 G(x - x', z)E^i(x')\exp(ik\cos\theta_0\Delta\theta x')\,\mathrm{d}x' + \int_2 G(x - x', z)E^i(x')\exp(ik\cos\theta_0\Delta\theta x')\,\mathrm{d}x', \quad (4)$$

and the indexes 1 and 2 at the signs of the integrals mean integration over the first and the second slits accordingly.

3. Double-slit dynamical diffraction

Let us consider the scheme given in Fig. 1. X-rays originating from a point source and passing through two slits fall on the crystal. The widths of the slits in the diffraction plane along the surface of the crystal are equal to each other and are equal to $2a$. The distance A_1B_2 from the left edge of the first slit to the right edge of the second slit is $2(c + a)$, *i.e.* the distance between the centres of the two slits is $2c$.

The boundaries of the regions, which are shown in Fig. 1, are formed by the lines A_1A_0, A_1B *etc.*, which are parallel to the directions of the transmitted and diffracted waves.

According to (4), the diffracted wave in the crystal is formed in the region $A_0B_0B_2A_1$. The amplitudes of the waves in the shaded triangle B_1A_2Q are equal to zero. An interference pattern of two slits is formed in the range Q_1AB (where both slits contribute to the amplitude of the diffracted wave with their whole widths $2a$) and is observed in the region AB of the exit surface of the crystal. In the parabolic approximation the amplitude of the incident wave for any polarization state (σ or π) and for any frequency is

$$\begin{aligned} E^i &= A\exp\left(ikx^2\cos^2\theta/2L_s\right)/L_s \\ &\equiv A\exp(ikx^2\cos^2\theta/2L_s), \end{aligned} \tag{5}$$

where L_s is the source–crystal distance. The amplitude E_h can be obtained by inserting (5) into (4). The expression for the amplitude is a coherent sum of two amplitudes E_{h1} and E_{h2}. E_{h1} is the amplitude of the diffracted wave emerging from slit 1 and E_{h2} is that emerging from slit 2. Thus,

$$E_h = E_{h1} + E_{h2}, \tag{6}$$

and

$$\begin{aligned} E_{h1} = A\int_{-c-a}^{-c+a} G(x-x',z)\exp(ikx'^2\cos^2\theta/2L_s) \\ \times\exp(ik\cos\theta_0 x'\Delta\theta)\,dx', \end{aligned} \tag{7}$$

$$\begin{aligned} E_{h2} = A\int_{c-a}^{c+a} G(x-x',z)\exp(ikx'^2\cos^2\theta/2L_s) \\ \times\exp(ik\cos\theta_0 x'\Delta\theta)\,dx'. \end{aligned} \tag{8}$$

3.1. Infinitely narrow slits (two coherent point sources on the entrance surface of the crystal)

The slits in Young's ideal experiment are considered as infinitely narrow and it is assumed that $c \gg a$. In the case of X-ray diffraction the slits can be regarded as infinitely narrow if $a \ll \Lambda\tan\theta_0/\pi$. This follows from (3), (7) and (8). In (7) and (8), Green's function is almost constant if $a \ll \Lambda\tan\theta_0/\pi$. The difference between the quadratic phase of $\exp(ikx'^2\cos^2\theta/2L_s)$ in the centre of the second slit and the right edge B_2 is approximately equal to $kac\cos^2\theta/L_s$. The quadratic phase in (8) can be considered as a constant if $kac\cos^2\theta/L_s \ll 2\pi$, *i.e.*

$$L_s \ll kac\cos^2\theta/2\pi. \tag{9}$$

The variation of the linear term of the phase in (8) from the left edge A_2 of slit 2 to the right edge B_2 is $k\cos\theta_0(2a)\Delta\theta$. This term can be considered constant if $|k\cos\theta_0(2a)\Delta\theta| \ll 2\pi$. Therefore,

$$|\Delta\theta| \ll \lambda/2a\cos\theta_0. \tag{10}$$

The same conditions (9) and (10) and the corresponding estimates are also true for slit 1. Then, the amplitude in the case of two infinitely narrow slits (two coherent point sources placed at the points $-c$ and c) can be rewritten using (6), (7) and (8) as

$$\begin{aligned} E_h = (2a)A\big[G(x+c,z)\exp(-ikc\cos\theta_0\Delta\theta) \\ + G(x-c,z)\exp(ikc\cos\theta_0\Delta\theta)\big]\exp(ikc^2\cos^2\theta/2L_s). \end{aligned} \tag{11}$$

For the distribution of the intensity on AB in the vicinity of the point $x = 0$ (the middle of AB) an approximate expression can be derived. Let us assume that

$$z\tan\theta_0 \gg |x \pm c| \tag{12}$$

and

$$\pi z/\Lambda_r \gg 1. \tag{13}$$

As is well known, the asymptotic behaviour of the Bessel function $J_0(x)$ in the case of $|x| \gg 1$ is

$$J_0(x) = (2/\pi x)^{1/2}\cos(x-\pi/4). \tag{14}$$

Using the conditions (12) and (13), the asymptotic presentation (14), the identity $\cos(x-\pi/4) = \{\exp[i(x-\pi/4)] + \exp[-i(x-\pi/4)]\}/2$, as well as the approximation $[z^2\tan^2\theta_0 - (x\pm c)^2]^{1/2} \simeq z\tan\theta_0[1-(x\pm c)^2/2z^2\tan^2\theta_0]$, the following expression can be obtained from (11),

$$\begin{aligned} E_h = i\sigma_h C(2a)A\left(2\Lambda/\pi^2 z\right)^{1/2}\exp(ik\chi_0 z/2\cos\theta_0) \\ \times\left[\exp(i\Phi_0)\cos(\Phi_+) + \exp(-i\Phi_0)\cos(\Phi_-)\right] \\ \times\exp\left(ikc^2\cos^2\theta/2L_s\right). \end{aligned} \tag{15}$$

The following notations in (15) are used: $\sigma_h = k\chi_h/4\sin\theta_0$, $\Phi_0 = (\pi z/\Lambda) - [\pi(x^2+c^2)/2\Lambda z\tan^2\theta_0] - \pi/4$; $\Phi_\pm = (\pi xc/\Lambda z\tan^2\theta_0) \pm kc\cos\theta_0\Delta\theta$.

As Λ is a complex quantity, the same is also true for Φ_0 and $\Phi_\pm$. The absorption near the middle of AB, from $x = 0$ to $|x| \geq c$, is associated with χ_{0i} in the term $\exp(ik\chi_0 z/2\cos\theta_0)$ and with Λ_i which can be taken into account only in $\exp(\pm i\Phi_0)$ in the term $\exp(\pm i\pi z/\Lambda)$ [according to conditions (12) and (13)]. As a result, for the absorption factor one obtains $\exp[-k\chi_{0i}(1\mp C\chi_{hi}/\chi_{0i})z/\cos\theta_0]$. Thus, in this region, the effective linear absorption coefficient coincides with that in the case of the plane incident wave (Authier, 2001; Pinsker, 1982): $\mu_e = \mu(1\mp C\chi_{hi}/\chi_{0i})$, where $\mu = k\chi_{0i}$ is the normal linear absorption coefficient and the sign $\mp$ corresponds to the sign $\pm$ in the term $\exp(\pm i\pi z/\Lambda)$. Thus, the first term in (15) corresponds to the weakly absorbing mode [with the effective linear absorption coefficient $\mu_e = \mu(1 - C\chi_{hi}/\chi_{0i}) < \mu$] and the second term corresponds to the strongly absorbing mode [with the effective linear absorption coefficient $\mu_e = \mu(1 + C\chi_{hi}/\chi_{0i}) > \mu$]. On the other hand, for the weakly absorbing mode, $\mu_{e\sigma} = \mu(1 - \chi_{hi}/\chi_{0i}) < \mu_{e\pi} = \mu(1 - \cos 2\theta_0\chi_{hi}/\chi_{0i})$. In the case $\mu z \geq 1$, only weakly absorbing modes of both polarizations can be taken into account, whereas in the case of sufficiently large $\mu z \gg 1$ only the weakly absorbing mode of σ polarization can be taken into account. For the weakly and strongly absorbing modes the maxima of the intensity distribution, according to (15), are defined from the conditions

$$(\pi xc/\Lambda_r z\tan^2\theta_0)\pm kc\cos\theta_0\Delta\theta = n\pi,\quad n=0,\pm1,\pm2\ldots. \tag{16}$$

The upper sign '+' on the left-hand side of (16) corresponds to the weakly absorbing mode. From (16) it follows that for both modes the periods are the same and are given as

$$D = \Lambda_r z\tan^2\theta_0/c. \tag{17}$$

Meanwhile the interference fringes of the weakly and strongly absorbing modes are shifted from the centre ($x = 0$) by

$$\Delta x = \mp kcD\cos\theta_0\Delta\theta/\pi. \tag{18}$$

The interference fringes obtained here are similar to Young's fringes in optics.

3.1.1. The influence of polarization on the interference pattern. According to (17) and (18) the periods D of Young's fringes for σ and π polarizations and the corresponding shifts Δx are different owing to the difference between $\Lambda_{r\sigma} = \lambda\cos\theta_0/|\chi_{hr}|$ and $\Lambda_{r\pi} = \Lambda_{r\sigma}/\cos2\theta_0$. Furthermore, the notations $D_\sigma = \Lambda_{r\sigma} z\tan^2\theta_0/c$ and $D_\pi = D_\sigma/\cos2\theta_0$ are used for the periods of Young's fringes for σ and π polarizations, respectively. The intensity of an unpolarized diffracted wave is the sum of the intensities of both polarizations. The intensities of strongly absorbing modes can be neglected ($\mu z \geq 1$). By using (16) and taking into account only weakly absorbing modes one obtains

$$\begin{aligned} I_h &= I_{h\sigma} + I_{h\pi} \\ &\simeq 2(2a)^2|A|^2\left(|\sigma_h|^2|\Lambda_\sigma|/\pi^2 z\right) \\ &\quad\times\left[\cos^2(kc\Delta\theta\cos\theta_0 + \pi x/D_\sigma)\right. \\ &\quad\left.+\cos2\theta_0\cos^2\left(kc\Delta\theta\cos\theta_0 + \pi x/D_\pi\right)\right]. \end{aligned} \tag{19}$$

The imaginary parts of the arguments of cosines are ignored. The expression (19) can be written as

$$\begin{aligned} I_h = (|\sigma_h|^2|\Lambda_\sigma|/\pi^2 z)(2a)^2|A|^2\{&(1+\cos2\theta_0) \\ &+(1+\cos2\theta_0)\cos[2kc\Delta\theta\cos\theta_0 + 2\pi x(1/D_\sigma + 1/D_\pi)/2] \\ &\times\cos[\pi x(1/D_\sigma - 1/D_\pi)] \\ &-(1-\cos2\theta_0)\sin[2kc\Delta\theta\cos\theta_0 + 2\pi x(1/D_\sigma + 1/D_\pi)/2] \\ &\times\sin[\pi x(1/D_\sigma - 1/D_\pi)]\}. \end{aligned} \tag{20}$$

The first term of (20) is constant. The third term is small since $\cos2\theta_0$ is close to 1. The second term is the main term. The second term has the period $[(1/D_\sigma + 1/D_\pi)/2]^{-1}$, which is slightly different from the periods of σ and π polarizations, D_σ and D_π. The intensity is modulated by the function $\cos[\pi x(1/D_\sigma - 1/D_\pi)]$. The interference fringes disappear if $\cos[\pi x(1/D_\sigma - 1/D_\pi)] = 0$, *i.e.*

$$(1-\cos2\theta_0)x/D_\sigma = (2n+1)/2. \tag{21}$$

The number of interference fringes between the two points of disappearance is

$$N = (1+\cos2\theta_0)/2(1-\cos2\theta_0). \tag{22}$$

3.1.2. Quasi-monochromatic radiation. The amplitudes of different components of a quasi-monochromatic incident beam are distributed in a small range, $\lambda\in(\lambda_m - \Delta\lambda_m, \lambda_m + \Delta\lambda_m)$ with $|\Delta\lambda/\lambda| \ll 1$. The wavelength λ_m corresponds to the component with maximal intensity. From differentiation of the Bragg formula one obtains

$$\theta_0(\lambda) - \theta_0(\lambda_m) = \Delta\lambda\tan\theta_0/\lambda, \tag{23}$$

and therefore

$$\begin{aligned} \Delta\theta(\lambda) &= \theta - \theta_0(\lambda) \\ &= \theta - \theta_0(\lambda_m) + \theta_0(\lambda_m) - \theta_0(\lambda) \\ &= \Delta\theta(\lambda_m) - \Delta\lambda\tan\theta_0/\lambda. \end{aligned} \tag{24}$$

Without loss of generality $\Delta\theta(\lambda_m) = 0$ and hence

$$\Delta\theta(\lambda) = -\Delta\lambda\tan\theta_0/\lambda. \tag{25}$$

From the condition (10) and the expression (25) it follows

$$\left|\Delta\lambda/\lambda\right| \ll \lambda/2a\sin\theta_0. \tag{26}$$

The shift of the interference pattern given by (18) is

$$\Delta x(\lambda) = \pm kcD\cos\theta_0\Delta\lambda\tan\theta_0/\pi\lambda. \tag{27}$$

From (17) it follows that $D_{\sigma,\pi} = D_{\sigma,\pi}(\lambda)$. Using (17) and (23) the following expressions are obtained:

$$\Delta D_\sigma(\lambda) = D_\sigma(\lambda)\left[(1+2\cos^2\theta_0)/\cos^2\theta_0\right]\Delta\lambda/\lambda, \tag{28}$$

$$\Delta D_\pi(\lambda) = D_\pi(\lambda)\left[(1+2\cos2\theta_0)/\cos^2\theta_0\cos2\theta_0\right]\Delta\lambda/\lambda. \tag{29}$$

Since $|\Delta\lambda/\lambda| \ll 1$ then $|\Delta D_{\sigma,\pi}(\lambda)| \ll D_{\sigma,\pi}(\lambda)$. Therefore the dependence of the periods on λ can be neglected. The conditions of the disappearance of interference fringes can be simply found. According to (18) the interference fringes corresponding to $\lambda_m - \Delta\lambda_m$ and $\lambda_m + \Delta\lambda_m$ are shifted with respect to each other by $2kcD\cos\theta_0\Delta\lambda_m\tan\theta_0/\pi\lambda$. If the maximum of zero order of $\lambda_m + \Delta\lambda_m$ coincides with the maximum of the first order of $\lambda_m - \Delta\lambda_m$, *i.e.* $2kcD\cos\theta_0\Delta\lambda_m\tan\theta_0/\pi\lambda = D$, the fringes disappear. Therefore the condition of the high visibility of the fringes is

$$\left|\Delta\lambda/\lambda\right| \ll \left|\Delta\lambda/\lambda\right|_{cr} = \pi/2kc\sin\theta_0 = \lambda/2(2c)\sin\theta_0. \tag{30}$$

Here, the subscript 'cr' denotes the critical value of $|\Delta\lambda/\lambda|$, at which the interference fringes disappear.

3.1.3. Source with finite size (spatial coherence). The finite size of the source can also affect the interference pattern. Let us consider a source of size l (Fig. 4). In the diffraction plane the source is a line perpendicular to the direction of the incident beam. The variable ξ indicates the coordinates of the point sources along the source. It varies from $-l/2$ to $l/2$. The glancing angle between the direction of the incident beam and the reflecting planes for a point source with coordinate ξ is $\theta(\xi) = \theta - \xi/L_s$. Therefore the deviation from Bragg's exact angle is

$$\Delta\theta(\lambda,\xi) = -(\Delta\lambda\tan\theta_0/\lambda) - \xi/L_s. \tag{31}$$

As follows from (31) and (18), for a fixed λ the incoherent point sources with the coordinates $\xi = -l/2$ and $\xi = l/2$ form sets of interference fringes shifted with respect to each other by $kc\cos\theta_0 lD/\pi L_s$. The interference fringes disappear when

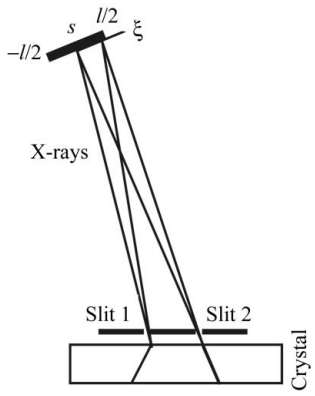

Figure 4
Scheme of double-slit dynamical diffraction for a source with finite size. *s*: X-ray source with finite size *l*.

$kc\cos\theta_0 lD/\pi L_s = D$. Therefore, the condition for observation of the interference fringes with high contrast is

$$l \ll \pi L_s/kc\cos\theta_0. \tag{32}$$

According to the Van Cittert–Zernike theorem (Born & Wolf, 2002), for homogeneous vacuum–slits and slits–vacuum media one can estimate

$$l \leq 0.16\pi L_s/kc\cos\theta_0. \tag{33}$$

In the Van Cittert–Zernike theorem, Green's function of a homogeneous medium is used, *i.e.* $\exp(ikR)/R$, where R is the distance between two points in the vacuum–slits and slits–vacuum spaces. It is interesting to note that the estimates [equations (32) and (33)] are almost the same, but in our case the vacuum–slits and slits–crystal medium is not homogeneous. For establishment of any theorem in our case similar to the Van Cittert–Zernike theorem it is necessary for the slits–crystal space to use the appropriate Green function.

3.2. Determination of the refractive index of a specimen (Rayleigh X-ray interferometer) and the angular distance of two incoherent sources (Michelson X-ray stellar interferometer)

The scheme given in Fig. 2 can be used for determination of the decrement δ of a specimen which is placed behind one of the slits (as for the Rayleigh interferometer in optics). The wave, passing the sample, placed in the way of slit 2, acquires an additional phase $-k\delta t$, where t is the thickness of the specimen. Therefore, instead of (18) (for weakly absorbing mode) we have

$$\Delta x = -(kcD\cos\theta_0\Delta\theta/\pi) + k\delta tD/2\pi,$$

and the shift $\Delta x(\delta)$, which is connected to the refraction in the specimen, is

$$\Delta x(\delta) = k\delta tD/2\pi. \tag{34}$$

By measuring $\Delta x(\delta)$ the refractive index of the specimen can be determined.

Using the scheme given in Fig. 3 makes it possible to determine the angular distance of two incoherent sources (as is done by means of the Michelson stellar interferometer in optics). Let us consider two incoherent sources. Sources emit plane waves ($L_s \to \infty$) that form glancing angles θ_1 and θ_2 with the reflecting planes. The total intensity distribution, according to (15) (the weakly absorbing mode), is

$$I_h \simeq 1 + \cos\big[(2\pi x/D) + k\cos\theta_0(\Delta\theta_1 + \Delta\theta_2)c\big] \times \cos\big[k\cos\theta_0(\Delta\theta_1 - \Delta\theta_2)c\big], \tag{35}$$

where $\Delta\theta_1 = \theta_1 - \theta_0$, $\Delta\theta_2 = \theta_2 - \theta_0$. By variation of c, the disappearance of the fringes can be achieved. For disappearance of the fringes, the condition $k\cos\theta_0|\theta_1 - \theta_2|c = \pi/2$ must be fulfilled. Then, the angular distance can be determined:

$$|\theta_1 - \theta_2| = \pi/2k\cos\theta_0 c. \tag{36}$$

3.3. Slits with finite size

The expressions (7) and (8) can be written in the form

$$E_{h1,2} = A\int_{-a}^{a} G(x \pm c - x', z)\exp\big[ik(x' \mp c)^2\cos^2\theta/2L_s\big] \times \exp\big[ik\cos\theta_0(x' \mp c)\Delta\theta\big]\,dx', \tag{37}$$

where the upper sign corresponds to slit 1 and the lower sign to slit 2. The expressions (37) cannot be integrated analytically. However, if the condition (13) is fulfilled, the asymptotic presentation (14) of the Bessel function can be applied. For the weakly absorbing mode one can find

$$E_{h1,2} = F_{1,2}(x, z)\int_{-a}^{a}\exp\big[i\pi(x \pm c)x'/\Lambda z\tan^2\theta_0\big] \times \exp(\mp ikx'c\cos^2\theta/L_s)\exp(ik\cos\theta_0 x'\Delta\theta)\,dx',$$

where

$$F_{1,2}(x, z) = iA(\sigma_h/2)C(2\Lambda/\pi^2 z)^{1/2}\exp(ik\chi_0 z/2\cos\theta_0) \times \exp(i\pi z/\Lambda)\exp(-i\pi/4) \times \exp(\mp ikc\cos\theta_0\Delta\theta) \times \exp\big[-i\pi(x^2 + c^2)/2z\Lambda\tan^2\theta_0\big] \times \exp(\mp i\pi xc/\Lambda z\tan^2\theta_0) \times \exp(ikc^2\cos^2\theta/2L_s).$$

In the integrand, quadratic terms of the phases dependent on x' are neglected ($ka^2\cos^2\theta/2L_s \ll \pi$, $a^2/2|\Lambda|z\tan^2\theta_0 \ll 1$). The remaining integrals correspond to the finite size of the slits. After integrations we obtain

$$E_{h1,2} = F_{1,2}(x, z)(2a)\sin\gamma_{1,2}/\gamma_{1,2}, \tag{38}$$

where

$$\gamma_{1,2} = ka\cos\theta_0[\Delta\theta \mp (c\cos\theta_0/L_s) + \pi(x \pm c)/k\Lambda z\tan^2\theta_0\cos\theta_0].$$

In the expressions of $\gamma_{1,2}$ the difference between $\cos\theta_0$ and $\cos\theta$ is neglected and for Λ only the real part Λ_r can be taken into account. From (38) and expressions for $\gamma_{1,2}$ it follows that the influence of the finite sizes of the slits can be neglected if

$$ka\cos\theta_0|\Delta\theta| \ll \pi,$$
$$kac\cos^2\theta_0/L_s \ll \pi, \quad (39)$$
$$\pi(|x|+c)a/cD \ll \pi.$$

The third condition in (39) is fulfilled independently of x if $\pi(|x_{\max}|+c)a/cD = \pi a/\Lambda_r \tan\theta_0 \ll \pi$. Here, $|x_{\max}| = AB/2$ (Fig. 1). The intensity distribution is given by the formula

$$I_h = \left|E_{h1} + E_{h2}\right|^2. \quad (40)$$

If the conditions (39) are fulfilled, the slits can be considered as infinitely narrow. The third condition of (39) in the region $|x| < c$ (particularly at $x = 0$) can be rewritten as $\pi ca/cD = \pi a/D \ll \pi$, *i.e.* $a \ll D$. This means that for appearance of the interference fringes the phase difference $\pi a/D$ between the centre of the slit and its ends must be less than π.

In general, the visibility of the fringes depends on the size of the slits. The main features of the influence of the finite size of the slits can be derived by analysing the behaviour of the functions $\sin\gamma_{1,2}/\gamma_{1,2}$. Let us analyse the behaviour of these functions neglecting the influence of absorption in their arguments. According to (38) the maxima of the functions $\sin\gamma_{1,2}/\gamma_{1,2}$ have coordinates

$$x_{\max 1,2} = \mp c - (kcD\cos\theta_0\Delta\theta/\pi) \pm kc^2\cos^2\theta_0 D/\pi L_s. \quad (41)$$

Here, the upper sign corresponds to slit 1. The first two zeros of the functions $\sin\gamma_{1,2}/\gamma_{1,2}$ have the coordinates

$$x_{01} = \pm(cD/a) - c - (kcD\cos\theta_0\Delta\theta/\pi) + kc^2\cos^2\theta_0 D/\pi L_s \quad (42)$$

for slit 1 and

$$x_{02} = \pm(cD/a) + c - (kcD\cos\theta_0\Delta\theta/\pi) - kc^2\cos^2\theta_0 D/\pi L_s \quad (43)$$

for slit 2. The $\pm$ signs in (42) and (43) correspond to $\sin\gamma_{1,2} = \pm\pi$. The distance between the maxima $\Delta x_{\max} = x_{\max 2} - x_{\max 1}$ is

$$\Delta x_{\max} = 2c(1 - kc\cos^2\theta_0 D/\pi L_s) \quad (44)$$

and does not depend on $\Delta\theta$. If $L_s = \infty$, $\Delta x_{\max} = 2c$. With a decrease of L_s, $\Delta x_{\max}$ decreases and $\Delta x_{\max} > 0$. The distance $\Delta x_{\max}$ is equal to zero when

$$L_{s0} = kc\cos^2\theta_0 D/\pi. \quad (45)$$

In this case, $x_{\max 1,2} = 0$ if $\Delta\theta = 0$. With a subsequent decrease of L_s, $|\Delta x_{\max}|$ increases, but now $\Delta x_{\max} < 0$. The interference occurs when the functions of the two slits have a region of overlap. The size of the overlapping region is maximal when the condition (45) is fulfilled. With increasing widths of the slits the distance between the two zeros of the slits' functions decreases. Consequently, with increasing width of the slits the area of overlap decreases.

Absorption introduces some corrections in the behaviour of the functions (38). Owing to absorption and the influence of quadratic terms, which are neglected in the phases of the integrands in (37) near the edges of AB, the absolute values of the coordinates of the first zeros of the separate slits' functions (37) and (38) are less than predicted by (42) and (43)

3.4. Example

Consider an example which illustrates the results obtained for the Si(220) Mo K_α reflection ($\lambda \simeq 0.7$ Å, $\theta_0 = 10.6^\circ$, $\Lambda_{r\sigma} = 36.6$ µm). The following parameters of the slits and the crystal are taken: $2c = 160$ µm, $2a = 10$ µm, $z = 3$ mm and the necessary silicon data

$$\chi_{0r} = -3.162\times10^{-6}, \quad \chi_{0i} = 0.165\times10^{-7},$$
$$\chi_{hr} = \chi_{\bar{h}r} = -1.901\times10^{-6}, \quad \chi_{hi} = \chi_{\bar{h}i} = 0.159\times10^{-7}$$

are taken from Pinsker (1982). For the chosen data, $\mu z = 4.4$, and therefore only the weakly absorbing modes of both polarizations can be taken into account.

In all the figures below, the intensity distribution is shown in the region AB at the exit surface of the crystal (Fig. 1) and, as a unit of intensity, the intensity of one of the polarization components of the incident unpolarized beam is taken, $I_0 = I_0^i/2 = |A|^2$, where I_0^i is the intensity of the incident beam.

It is necessary to discuss all conditions of visibility of the fringes. The condition (10) is similar to the first condition of (39). For the case under consideration one can estimate from (39) that for the visibility of the fringes of infinitely narrow slits the fulfilment of the condition $|\Delta\theta| \ll 7.2\times10^{-6}$ is necessary. On the other hand, the temporal coherence length is restricted by the conditions (26) and (30). However, if the condition (30) occurs, the condition (26) is fulfilled automatically. From the condition (30) the estimate $|\Delta\lambda/\lambda| \ll 1.2\times10^{-6}$ is obtained. The second condition of (39) gives an estimate of the collimation degree of the incident beam concerned with the finite size of the slits. From (39) it follows that $L_s \gg 22$ m. The third condition of (39) is not satisfied near the edges of AB as $a/\Lambda_{r\sigma}\tan\theta_0 = 0.73$.

The spatial coherence, *i.e.* the effect of the source with finite size, is estimated from (32). If the size of the source is $l = 30$ µm, then from (32) we obtain $L_s \gg 70$ m. Thus, the beam must be collimated so that the collimation degree corresponds to $L_s \gg 70$ m. According to (22), the modulation, owing to polarization, arises when the number of fringes is $N = 14$. The period is a function of the observation depth. At $z = 3$ mm, for the period of both polarizations the values $D_\sigma = 48.3$ µm, $D_\pi = 51.8$ µm can be obtained [see formula (17)]. Fig. 5 shows that the main obtained results are consistent with the numerical calculations. It also shows the modulation of the fringes owing to summation by polarizations. The results of numerical calculations are in good agreement with those obtained from (17).

As has been shown above, the interference fringes disappear when $|\Delta\lambda/\lambda| = \left|\Delta\lambda/\lambda\right|_{cr} = 1.2\times10^{-6}$ [according to (30)]. This is shown in Fig. 6(*a*). For the source with finite size, the fringes disappear for the distance $L_{s\,cr} = kc\cos\theta_0 l/\pi = 70$ m [formula (32)]. The numerical calculations (Fig. 6*b*) agree with this result.

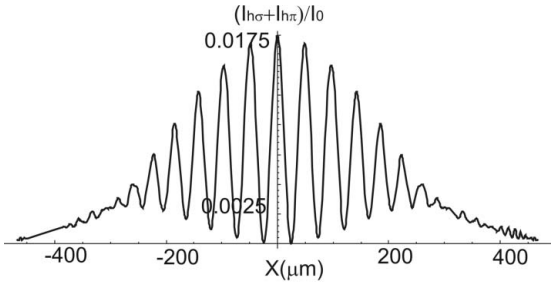

Figure 5
Intensity distribution in the region AB for a plane incident unpolarized monochromatic wave ($I_h = |E_{h\sigma}|^2 + |E_{h\pi}|^2$, $L_s = \infty$, $\Delta\theta = 0$). Numerical calculations are based on the formulae (7), (8) and (40).

According to Fig. 7 the approximations for separate slits [formula (38)] give a result very close to the results obtained by numerical calculations [formula (37)].

The intensity distributions of the interference fringes corresponding to the cases in Figs. 7 and 8(*a*) are shown in Figs. 5 and Fig. 8(*b*). Comparison of Figs. 8(*b*) and 5 shows that the interference fringes disappear for the slits with the larger widths. The region of overlap of the slits' functions for Fig. 8(*a*) is small. In Fig. 9(*a*) it is seen that the slits' functions are

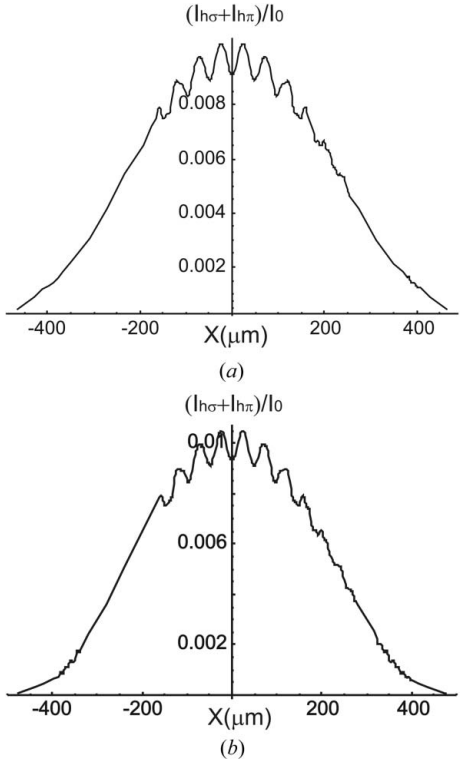

Figure 6
(*a*) Intensity distribution for quasi-monochromatic radiation. $\Delta\lambda/\lambda = (\Delta\lambda/\lambda)_{cr} = 1.2 \times 10^{-6}$. Numerical calculations are based on formulae (7) and (40) with subsequent integration of intensity by $\Delta\lambda$ and polarizations. The intensity distribution on λ of the incident beam is considered constant. (*b*) Interference fringes for a source with finite size $l = 30$ μm in the diffraction plane. $L_s = L_{s\,cr} = 70$ m. Numerical calculations are based on formulae (7), (8) and (40) with subsequent integration of intensity by ξ and polarizations.

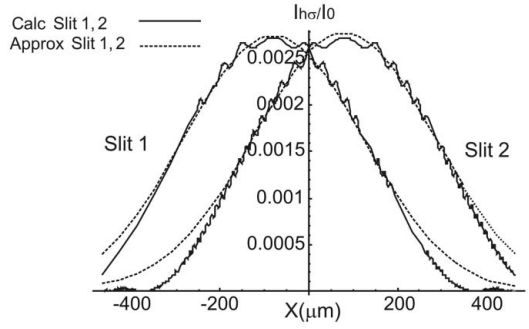

Figure 7
Intensity distributions of separate slits ($L_s = \infty$, $\Delta\theta = 0$, $\Delta\lambda = 0$, σ polarization) obtained by numerical calculations on the basis of formula (37) and the intensity distributions obtained by means of the approximated formula (38).

maximally overlapped for $L_s = kc\cos^2\theta_0 D/\pi$. Comparison of Figs. 8(*b*) and 9(*b*) shows that at this distance the interference pattern appears again. The number of fringes in Fig. 9(*b*) is smaller in comparison with the case when $2a = 10$ μm because the half-width of the slits' functions are smaller in the case when $2a = 45$ μm.

Finally, let us estimate the angular distance between two incoherent sources, which can be determined by means of the Michelson dynamic diffraction stellar interferometer. According to (37), $|\theta_1 - \theta_2| = 0.05''$. Since the distance c can be taken greater, the angular distance can be measured with greater accuracy.

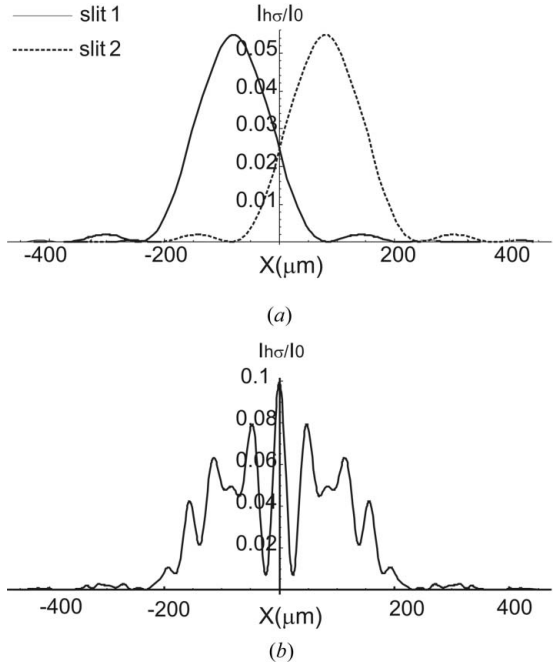

Figure 8
(*a*) The intensity distributions for separate slits. σ polarization, plane monochromatic wave, $\Delta\theta = 0$, $2a = 45$ μm. Numerical calculation by formula (37). (*b*) Corresponding double-slit interference fringes. Numerical calculation.

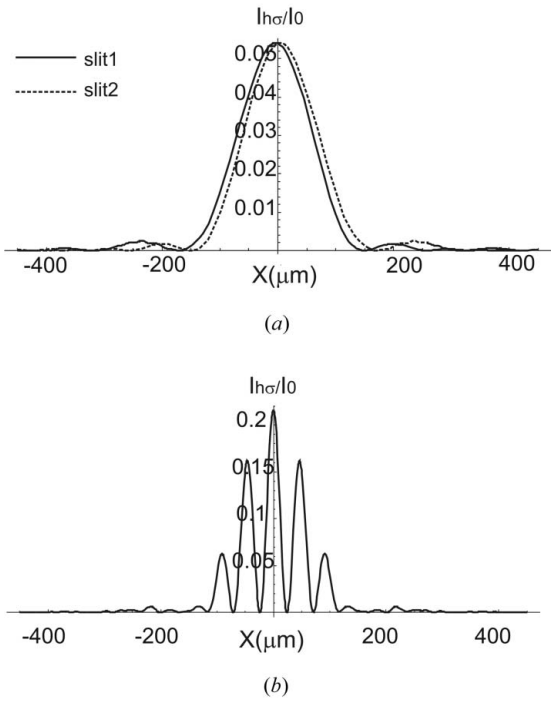

Figure 9
Intensity distributions for separate slits (*a*) and double-slit interference fringes (*b*) corresponding to σ polarization, spherical monochromatic wave, $L_s = L_{s0} = 105.5$ m, $\Delta\theta = 0$, $2a = 45$ μm. Numerical calculation.

4. Conclusions

4.1. Results

In this paper the following results have been obtained.

(i) The double-slit dynamical diffraction of X-rays in perfect crystals is theoretically investigated. It is shown that interference fringes are formed on the exit surface of the crystal. These fringes are similar to Young's fringes and the suggested scheme is similar to Young's double-slit experiment. Formulae for the period and for the intensity distribution of the interference fringes are obtained.

(ii) The influence of various factors on the characteristics of the interference fringes is investigated.

(iii) An example of theoretical results is considered for illustration. The numerical calculations agree with theoretical predictions.

4.2. Applications and further developments

The following applications and further developments are pointed out.

(i) The double-slit dynamical diffraction scheme can be used as an interferometer with a wavefront division (Rayleigh X-ray interferometer; Fig. 2). It is possible to determine the refractive index of a specimen which is placed in the path of a wave emerging from one of the slits.

(ii) The proposed scheme can be used as a Michelson X-ray stellar interferometer for measuring the angular distances between two incoherent sources (Fig. 3). Using the scheme given in Fig. 3 in X-ray astronomy is also possible.

(iii) The determination of localized defects in the crystal can be one of the applications of the scheme shown in Fig. 1. If one of the beams passes through the region of the crystal containing the localized defects (dislocations, plane defects *etc.*), the interference pattern must change. In principle, by analysing the recorded changes in the interference pattern it is possible to conduct at least a qualitative analysis of crystal defects. The theoretical and experimental investigation of double-slit dynamical diffraction in elastically deformed crystals is also interesting, *e.g.* bent crystals, crystals under the influence of a temperature gradient or ultrasonic waves *etc.*

(iv) The double-slit experiment in optics is one of the simplest ways to record holograms (Hariharan, 2002). It is obvious that the scheme given in Fig. 1 is a way of recording an X-ray hologram of a point source. The subsequent reconstruction of the image by visible light is also possible. Thus, a further theoretical and experimental development of the proposed scheme could be X-ray holography. By placing an object in one of the slits it is possible to record an X-ray hologram of the object. Such a method in X-ray optics is similar to Fourier lensless holography in optics.

(v) The theoretical and experimental investigation of double-slit dynamical diffraction also seems to be interesting in the case of Bragg geometry of diffraction.

4.3. Possibility of experimental realization

According to the estimates of the monochromatization degree [formula (30)] and the source size [formula (32)] of the incident beam it is more convenient to use a synchrotron radiation source rather than a laboratory source of X-rays. One of the possible experimental setups for incident beam formation could be the same as that of beam formation given by Yamazaki & Ishikawa (2003), where interference fringes of a three-block X-ray wavefront-division Laue interferometer have been demonstrated. The experimental setup for incident beam preparation has the following components: double-crystal monochromator + asymmetric cut crystal collimator. The asymmetric collimator has an asymmetry factor from 1/50 to 1/10. For experimental realization of the double-slit dynamical diffraction one must replace the three-block interferometer by the double slit + crystal system. It is possible that the use of a laboratory X-ray source with the corresponding asymmetric crystal collimator can provide an opportunity for experimental investigations with two slits.

The author is grateful to Dr L. G. Gasparyan and Dr V. P. Mkrtchyan for helpful discussions on the possibility of the experimental realization of double-slit dynamical diffraction.

References

Als-Nielsen, J. & McMorrow, D. (2001). *Elements of Modern X-ray Physics.* Chichester: John Wiley and Sons.
Authier, A. (2001). *Dynamical Theory of X-ray Diffraction.* Oxford University Press.

Authier, A., Malgrange, C. & Tournarie, M. (1968). *Acta Cryst.* A**24**, 126–136.
Authier, A. & Simon, D. (1968). *Acta Cryst.* A**24**, 517–526.
Born, M. & Wolf, E. (2002). *Principles of Optics*, 7th ed. Cambridge University Press.
Hariharan, P. (2002). *Basics of Holography*. Cambridge University Press.
Hart, M. & Milne, A. D. (1968). *Phys. Status Solidi*, **26**, 185–189.
Homna, Sh., Ando, Yo. & Kato, N. (1966). *J. Phys. Soc. Jpn*, **21**, 1160–1165.
Isakovic, A. F., Stein, A., Warren, J. B., Sandy, A. R., Narayanan, S., Sprung, M., Ablett, J. M., Siddons, D. P., Metzler, M. & Evans-Lutterodt, K. (2010). *J. Synchrotron Rad.* **17**, 451–455.
Kato, N. (1961*a*). *Acta Cryst.* **14**, 526–532.
Kato, N. (1961*b*). *Acta Cryst.* **14**, 627–636.
Kato, N. (1968*a*). *J. Appl. Phys.* **39**, 2225–2230.
Kato, N. (1968*b*). *J. Appl. Phys.* **39**, 2231–2237.
Kato, N. & Lang, A. R. (1959). *Acta Cryst.* **12**, 787–794.
Kohra, K. & Kikuta, S. (1968). *Acta Cryst.* A**24**, 200–205.
Leitenberger, W., Kusnetsov, S. M. & Snigirev, A. (2001). *Opt. Commun.* **191**, 91–96.
Leitenberger, W. & Pietsch, U. (2007). *J. Synchrotron Rad.* **14**, 196–203.
Leitenberger, W., Wendrock, H., Bischoff, L. & Weitkamp, T. (2004). *J. Synchrotron Rad.* **11**, 190–197.
Pinsker, Z. G. (1982). *X-ray Crystal Optics*. Moscow: Nauka (In Russian.)
Slobodetskii, I. Sh. & Chukhovskii, F. N. (1970). *Kristallografiya*, **15**, 1101–1107.
Slobodetskii, I. Sh., Chukhovskii, F. N. & Indenbom, V. L. (1968). *ZhETF Pis. Red.* **8**, 90–94.
Takagi, S. (1969). *J. Phys. Soc. Jpn*, **26**, 1239–1253.
Tsuji, T., Koyama, H., Takano, Y. & Kagoshima, Y. (2009). *J. Phys. Conf. Ser.* **186**, 012061.
Uragami, T. (1969). *J. Phys. Soc. Jpn*, **27**, 147–154.
Yamazaki, H. & Ishikawa, T. (2003). *J. Appl. Cryst.* **36**, 213–219.